

# Impact of loading frequency and consolidation level on the mechanical behaviors of saturated clayey soils under cyclic loading

Jang-Un Kim, So Young Kim, Jeong Woo Kim, Chan Kim, Hyunwook Choo

Department of Civil and Environmental Engineering, Hanyang University, Seoul, South Korea, choohw@hanyang.ac.kr

**ABSTRACT:** Saturated clayey soils are often subjected to cyclic loading at varying loading frequencies ( $f_c$ ) due to natural or anthropogenic causes. However, the combined influence of cyclic frequency and the initial consolidation level ( $U_i$ ) on soil behavior remains not fully understood. This study investigates the mechanical response of saturated kaolin clays with different initial consolidation levels ( $U_i = 0$  to 1.0) subjected to cyclic loading frequencies ranging from 0.011 to 250 mHz under  $K_\theta$  conditions. A custom-designed cyclic loading system, comprising a cyclic loading cylinder and a modified oedometer cell, was employed to apply a sequence of monotonic loading ( $\sigma'_v = 2.2$  to 100 kPa), cyclic loading (100 to 200 kPa), additional monotonic loading (200 to 300 kPa), and unloading (300 to 50 kPa) phases. Throughout these phases, additional volume change ( $\Delta e$ ), lateral stress ( $\sigma'_h$ ), and shear wave velocity ( $V_s$ ) were continuously monitored. Results demonstrate that for specimens with a low initial consolidation level ( $U_i \approx 0$ ), accumulated  $\Delta e$  during cyclic loading increased significantly with increasing  $f_c$ . This increase is attributed to elevated excess pore water pressure and the consequent reduction in effective stress and inter-particle frictional resistance. As  $U_i$  increased, the sensitivity of  $\Delta e$  to  $f_c$  variations diminished, demonstrating the stabilizing effect of consolidation. A critical finding of this study was the existence of  $f_c$  thresholds related to the loading period ratio, ( $LPR = T/t_{100}$ , where  $T$  is the cyclic period and  $t_{100}$  is the duration for full primary consolidation). When  $LPR > 1.0$  (pseudo-drained state) or  $LPR \leq 0.001-0.01$  (pseudo-undrained state), the influence of  $f_c$  on the mechanical properties of tested clays with varying  $U_i$  became negligible. Additionally, changes in  $\sigma'_h$  and  $V_s$  during cyclic loading are reported, providing further insight into the microstructural response of tested clays under varying loading conditions.

**KEYWORDS:** Cyclic loading; Saturated soil; Lateral stress; Shear wave velocity; Mechanical properties.

## 1 INTRODUCTION

Saturated clay is characterized by high compressibility and low permeability, experiences cyclic loading with a broad frequency range ( $f_c = 0.01-10,000$  mHz) due to both natural and anthropogenic factors (Vucetic and Dobry, 1988; Pasten and Carlos Santamarina, 2011). Understanding the compressibility response of such soils under cyclic loading is essential for evaluating the long-term stability of geotechnical structures. Previous research has identified key factors affecting the accumulation of plastic strain in soils subjected to cyclic loading, including soil type, initial void ratio, stress amplitude ratio, and the number of loading cycles (Wichtmann, 2005; Park and Santamarina, 2019; Ryu et al., 2022). Despite these findings, two critical issues remain unresolved:

(1) Limited consideration of cyclic loading frequency ( $f_c$ ): Cyclic loads in both natural and engineered environments cover a wide range of frequencies, necessitating comprehensive studies across this spectrum. However, prior investigations have predominantly focused on either high or low frequencies, leaving a significant gap in understanding the full frequency range.

(2) Different consolidation states: In-situ soils may exhibit spatially varying consolidation states even within the same stratigraphic layer due to geological processes such as consolidation, erosion, and re-deposition (Sangrey et al., 1979; Sun et al., 2015). This heterogeneity in consolidation makes it challenging to predict soil response under cyclic loading, leading to significant engineering challenges such as excessive settlement and reduced stability under cyclic loads.

As a result, these two issues reflect complex behavioral differences driven by distinct physical mechanisms, increasing the uncertainty in predicting soil response under cyclic loading. Moreover, while most of the aforementioned studies have been conducted under the assumption of either fully drained or undrained conditions, partially drained conditions are more representative of actual field environments. Therefore, this study aims to evaluate the mechanical behavior of saturated soils under various cyclic loading frequencies ( $f_c = 0.011, 0.046, 0.139, 0.28, 1.67, 8.33, 25, 125, \text{ and } 250$  mHz) and initial consolidation levels ( $U_i = 0, 0.2, 0.4, 0.6, \text{ and } 1.0$ ).

## 2 EXPERIMENTAL PROGRAM

### 2.1 MATERIALS

In this study, K-7 sand (Kyung In Material Company, South Korea) and kaolin clay (Lakwo Company, South Korea) were used as experimental materials under cyclic load application. According to the Unified Soil Classification System (USCS), K-7 sand was classified as poorly graded sand (SP), while kaolin clay was categorized as low plasticity clay (CL). The material properties of the tested materials are detailed in Table 1.

Table 1. Material properties of tested materials

Index properties	K-7 sand <sup>1)</sup>	Kaolin clay <sup>2)</sup>	Testing method
Specific gravity	2.65	2.53	ASTM D854
Median particle size ( $\mu\text{m}$ )	800.0	3.96	<sup>1)</sup> ASTM D7928 <sup>2)</sup> ASTM E3340
Uniformity coefficient	1.47	6.58	E3340
Liquid limit (%)	NP	38.4	BS-1377 (1990)
Plastic limit (%)	NP	23.6	ASTM D4318
End of primary consolidation time $t_{100}$ (sec)	132	4,284	ASTM D2435
Specific surface, $S_a$ ( $\text{m}^2/\text{g}$ )	0.03	10.92	Methylene blue (Santamarina et al., 2002)

## 2.2 EXPERIMENTAL EQUIPMENT

The cyclic loading system (Figure 1) consists of a pneumatic cylinder, a reaction frame, a pressure panel, and a modified oedometer cell to monitor void ratio changes under cyclic loading. The modified oedometer cell was designed to monitor changes in the void ratio ( $\Delta e$ ) during cyclic loading cycles under zero-lateral strain conditions, while a diaphragm transducer measured the horizontal effective stress ( $\sigma'_h$ ) and a pair of bender elements installed at the top and bottom of the cell measured the shear wave velocity ( $V_s$ ). The system controls stress precisely using synchronized input and feedback signals, maintaining pressure differences within 0.5%. The cyclic loading period ( $T$ ) can be set from a minimum of 4 seconds ( $f_c = 250$  mHz) to a maximum of 24 hours ( $f_c = 0.011$  mHz), and is verified through the measured responses of the load cell and pressure transducer during cyclic loading (Figure 1).

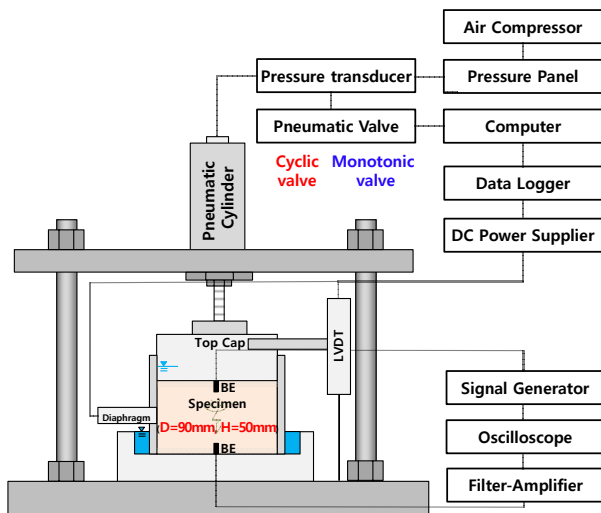


Figure 1. Experimental setup for tested materials during the cyclic mechanical loading.

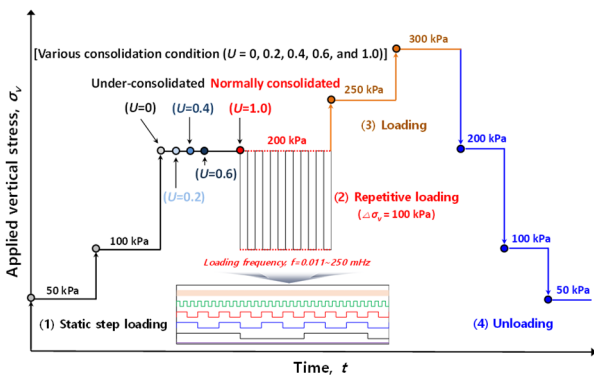


Figure 2. Applied vertical stress history for tested soils under various consolidation levels ( $U_i = 0, 0.2, 0.4, 0.6,$  and  $1.0$ )

## 2.3 SAMPLE PREPARATION AND PROGRAM

The study used oven-dried K-7 sand and kaolin clay mixed with deionized water. K-7 sand specimens were prepared through the water pluviation method to achieve an initial relative density ( $D_r$ ) of approximately 50%. Kaolin specimens were prepared using the slurry mixing method, with an initial water content set to 1.2 times the liquid limit. Before placement into the cell, the slurry was sealed in plastic wrap and stored in a humidity chamber for 72 hours to ensure uniform water distribution. All

specimens remained fully submerged during testing to maintain saturated conditions.

The loading sequence included monotonic loading ( $\sigma'_v$  ranging from 2.2–100 or 2.2–200 kPa), cyclic loading ( $\sigma'_v = 100$ –200 kPa with a cyclic stress amplitude of 100 kPa and cyclic loading numbers ( $N$ ) varying from  $10^2$  for  $T = 24$  hours to  $2 \times 10^4$  for  $T = 4$  seconds), an additional monotonic loading (maximum vertical stress,  $\sigma'_{v(max)} = 300$  kPa), and a final unloading ( $\sigma'_v$  ranging from 300 to 50 kPa) (Figure 2). In particular, the initial consolidation levels for the saturated clayey soils were controlled to represent various consolidation states, with  $U_i = 0, 0.2, 0.4, 0.6,$  and  $1.0$  under a monotonic vertical stress of 200 kPa (Figure 2).

## 3 RESULTS AND DISCUSSION

### 3.1 DEFORMATION CHARACTERISTICS

#### 3.1.1 EFFECT OF LOADING FREQUENCY

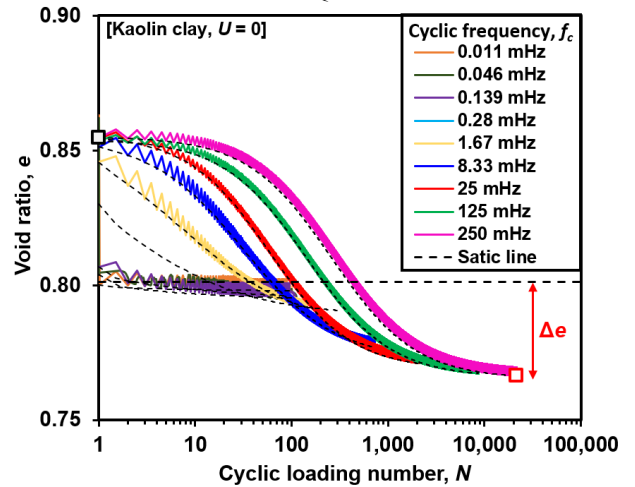


Figure 3. Variation in void ratio ( $e$ ) with cyclic loading number ( $N$ ) at different cyclic frequencies ( $U_i = 0$ ).

Figure 3 illustrates the variation in void ratio ( $e$ ) as a function of the cyclic loading number ( $N$ ) under a constant cyclic stress range of 100–200 kPa for kaolin clay with an initial consolidation level  $U_i = 0$ . As the cyclic loading frequency ( $f_c$ ) increases, the additional volume change ( $\Delta e = e_{monotonic} - e_{cyclic}$ ) increases, indicating that deformation accumulation under cyclic loading is highly sensitive to  $f_c$ . In particular, when compared to the static (or monotonic) loading condition (represented by the dashed line),  $\Delta e$  was 0.0047 at the lowest frequency ( $f_c = 0.011$  mHz) and 0.0331 at the highest frequency ( $f_c = 250$  mHz).

#### 3.1.2 EFFECT OF CONSOLIDATION LEVEL

Figure 4 shows the variation in void ratio ( $e$ ) with the cyclic loading number ( $N$ ) for different initial consolidation level ( $U_i$ ) under a cyclic frequency of  $f_c = 250$  mHz. As the initial consolidation level increases, the additional volume change ( $\Delta e$ ) tends to decrease. This is because structurally more stable specimens are subjected to cyclic loading after the dissipation of excess pore water pressure ( $U_i = 1.0$ ), resulting in minimal additional pore pressure buildup. Consequently, effective stress remains relatively stable, and structural changes are limited. Nevertheless, if the repeated strain exceeds the threshold for elastic deformation, the tested soils may exhibit progressive accumulation of volumetric strain under cyclic loading (Santamarina et al., 2019).

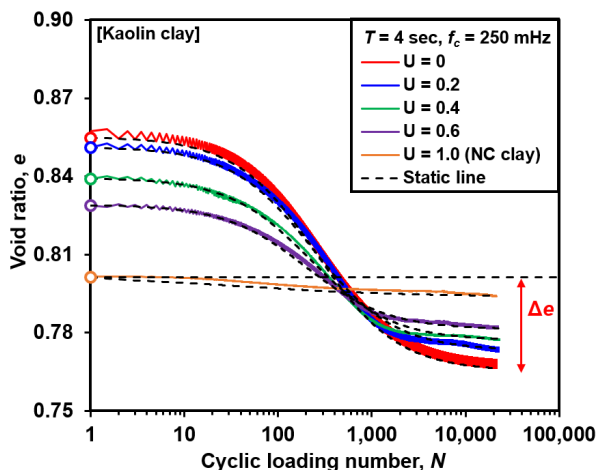


Figure 4. Variation in void ratio ( $e$ ) with cyclic loading number ( $N$ ) at different initial consolidation levels ( $f_c = 250$  mHz).

### 3.1.3 LOADING PERIOD RATIO

Figure 5(a) shows the additional volume change ( $\Delta e$ ) as a function of loading frequency ( $f_c$ ) for saturated K-7 sand and clayey soil specimens with varying initial consolidation levels ( $U_i$ ). Where,  $\Delta e$  represents the additional volumetric contraction induced by cyclic loading ( $\sigma'_v = 100\text{--}200$  kPa), and is defined as the difference in void ratio between monotonic and cyclic loading conditions ( $\Delta e = e_{\text{monotonic}} - e_{\text{cyclic}}$ ). Saturated K-7 sand and normally consolidated clayey soils ( $U_i = 1.0$ ) exhibited nearly constant  $\Delta e$  values across the frequency range of  $f_c = 0.011\text{--}250$  mHz, indicating frequency-independent behavior. In contrast, underconsolidated kaolin clays with  $U_i < 1.0$  exhibited frequency-dependent behavior, with  $\Delta e$  remaining relatively constant at low frequencies ( $f_c < 0.278$  mHz) regardless of the initial consolidation level. However, beyond  $f_c = 0.278$  mHz, all specimens exhibited a pronounced increase in  $\Delta e$ , indicating a transition behavior. This suggests that the compressibility of saturated clay under cyclic loading may drastically change beyond a certain threshold frequency. To further interpret this transition, the concept of the loading period ratio, defined as the ratio between the loading period ( $T$ ) and the excess pore water pressure dissipation time ( $t_{100}$ ), was introduced:

$$\text{Loading period ratio (LPR)} = \frac{T}{t_{100}} \quad (1)$$

where,  $t_{100}$  is the time required for 100% primary consolidation, obtained from the  $e\text{--}\log t$  curve.

Figure 5(b) illustrates the relationship between  $\Delta e$  and  $T/t_{100}$  for saturated K-7 sand and kaolin clay with various initial consolidation levels ( $U_i = 0$  to 1.0). K-7 sand and normally consolidated clays ( $U_i = 1.0$ ), changes in  $\Delta e$  were negligible with varying  $LPR$ . In contrast, clay specimens with  $U_i < 1.0$  exhibited a nonlinear increase in  $\Delta e$  as  $LPR$  decreased below 1.0. Particularly, the loading frequency at which  $\Delta e$  began to increase ( $f_c = 0.278$  mHz) corresponds to  $LPR = 0.906$ , suggesting that  $LPR \approx 1.0$  serves as a transition threshold for volume change characteristics under cyclic loading. Furthermore, under conditions of  $LPR > 1.0$  (pseudo-drained state) or  $LPR \leq 0.001\text{--}0.01$  (pseudo-undrained state), the influence of loading frequency ( $f_c$ ) on the mechanical behavior of clays with varying consolidation states becomes negligible.

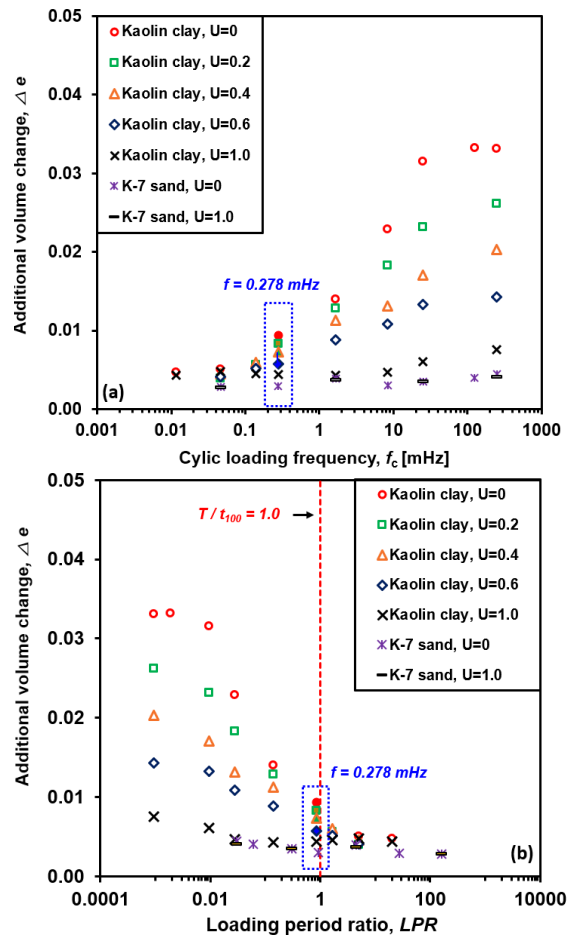


Figure 5. Change in additional volume change ( $\Delta e = e_{\text{monotonic}} - e_{\text{cyclic}}$ ) as a function of (a) cyclic loading frequency ( $f_c$ ) and (b) loading period ratio ( $LPR = T/t_{100}$ ).

### 3.2 LATERAL STRESS DURING CYCLIC LOADING

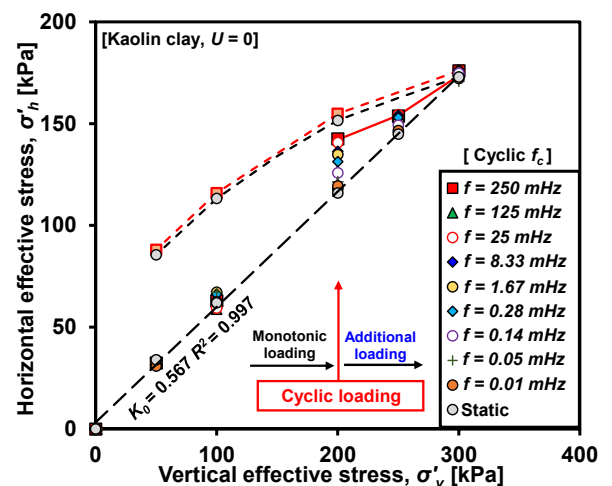


Figure 6. Variation of horizontal effective stress ( $\sigma'_h$ ) with vertical effective stress ( $\sigma'_v$ ) under different cyclic loading frequencies for kaolin clay ( $U_i = 0$ ).

Figure 6 presents the horizontal effective stress ( $\sigma'_h$ ) measured during the monotonic–cyclic–additional monotonic–unloading sequence with vertical effective stress ( $\sigma'_v$ ) under various cyclic frequency ( $f_c$ ). In the monotonic loading phase, the measured  $\sigma'_h$  increased almost linearly with increasing vertical effective

stress ( $\sigma'_v$ ), indicating that the coefficient of lateral earth pressure at rest ( $K_0 = \sigma'_h / \sigma'_v$ ) remained approximately constant at 0.567. However, during the cyclic loading phase,  $\sigma'_h$  values were higher than those recorded in the monotonic loading phase. At  $f_c = 250$  mHz, the  $K_0$  value increased to 0.722, representing a 27.3% increase compared with the monotonic loading condition. This phenomenon can be explained by the repeated separation of interparticle contacts under cyclic loading, which diminishes the internal frictional resistance and thereby facilitates the transfer of greater stresses in the horizontal direction (Han et al., 2024).

### 3.3 SHEAR WAVE VELOCITY DURING CYCLIC LOADING

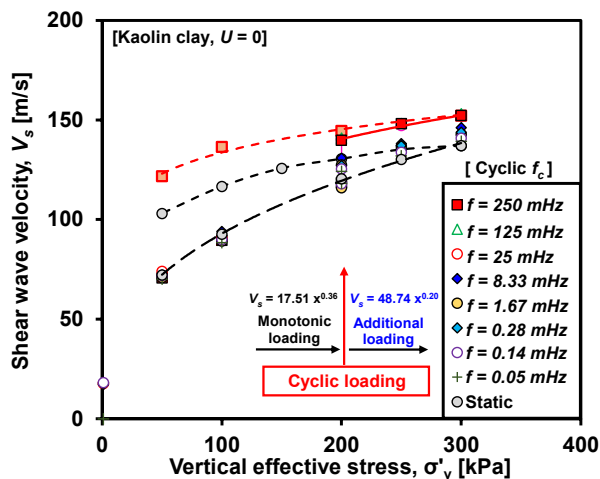


Figure 7. Variation of shear wave velocity ( $V_s$ ) with vertical effective stress ( $\sigma'_v$ ) under different cyclic loading frequencies ( $f_c$ ) for kaolin clay ( $U_i = 0$ )

Figure 7 illustrates the variation of shear wave velocity ( $V_s$ ) with vertical effective stress ( $\sigma'_v$ ) as a function of cyclic loading frequency ( $f_c$ ). Under monotonic loading without cyclic loading,  $V_s$  increased with increasing  $\sigma'_v$ , following a power function relationship. However, during the cyclic loading phase,  $V_s$  increased with increasing  $f_c$  at a  $\sigma'_v = 200$  kPa. The shear wave velocity in granular materials is governed by interparticle contact and interparticle coordination (Choo and Lee, 2021). An increase in applied stress enlarges the contact area between particles, which in turn enhances interparticle contact stiffness. Therefore, the increase in  $V_s$  observed during the cyclic loading phase can be attributed to the increase in horizontal effective stress. Moreover, during the unloading phase, unlike the horizontal effective stress data (Figure 6), the influence of  $f_c$  on fabric changes was captured more distinctly (Figure 7).

## 4 CONCLUSIONS

This experimental study aims to evaluate the compressibility of saturated clay under cyclic loading conditions with varying initial consolidation levels ( $U_i$ ) and loading frequencies ( $f_c$ ). The experimental results demonstrated that additional volumetric contraction ( $\Delta e$ ) increased with cyclic frequency ( $f_c$ ) and decreased with initial consolidation level ( $U_i$ ), with underconsolidated ( $U_i = 0$ ) specimens showing the greatest frequency sensitivity. A loading period ratio ( $LPR$ ) of approximately 1.0 was identified as a threshold separating frequency-dependent and frequency-independent deformation responses, with negligible  $f_c$  effects observed in pseudo-drained ( $LPR > 1.0$ ) and pseudo-undrained ( $LPR \leq 0.001-0.01$ ) states. Cyclic loading increased the horizontal effective stress ( $\sigma'_h$ ) by up to 27.3% compared with monotonic loading, leading

to enhanced shear wave velocity ( $V_s$ ) due to increased interparticle contact stiffness. These findings highlight the need to account for both cyclic loading frequency and consolidation level when assessing the mechanical response of saturated clays under cyclic loading.

## 5 ACKNOWLEDGEMENTS

This research was supported by the National Research Foundation of Korea (NRF) grant funded by the Korean government (MSIT). (RS-2023-00208844 and RS-2023-00221719).

## 6 REFERENCES

- Choo, H. and Lee, C., 2021. Inverse effect of packing density on shear wave velocity of binary mixed soils with varying size ratios. *Journal of Applied Geophysics*, 194, p.104457. <https://doi.org/10.1016/j.jappgeo.2021.104457>
- Han, H., Choo, H. and Park, J., 2024. Evaluation of the coefficient of lateral stress at rest of granular materials under repetitive loading conditions. *Journal of Rock Mechanics and Geotechnical Engineering*, 16(5), pp.1709–1721. <https://doi.org/10.1016/j.jrmge.2023.07.024>
- Park, J. and Santamarina, J.C., 2019. Sand response to a large number of loading cycles under zero-lateral-strain conditions: evolution of void ratio and small-strain stiffness. *Geotechnique*, 69(6), pp.501–513. <https://doi.org/10.1680/jgeot.17.P.268>
- Pasten, C. and Santamarina, J.C., 2011. Energy geo-storage—analysis and geomechanical implications. *KSCCE Journal of Civil Engineering*, 15(4), pp.655–667. <https://doi.org/10.1007/s12205-011-0006-6>
- Ryu, B., Choo, H., Park, J. and Burns, S.E., 2022. Stress–deformation response of rigid–soft particulate mixtures under repetitive  $K_0$  loading conditions. *Transportation Geotechnics*, 37, p.100835. <https://doi.org/10.1016/j.trgeo.2022.100835>
- Sangrey, D., Clukey, E. and Molnia, B., 1979. Geotechnical engineering analysis of underconsolidated sediments from Alaska coastal waters. In: *Proceedings of the Offshore Technology Conference (OTC)*. Houston, Texas, 30 April–3 May 1979. Richardson, Texas: Offshore Technology Conference.
- Santamarina, J.C., Park, J., Terzariol, M., Cardona, A., Castro, G.M., Cha, W., Garcia, A., Hakiki, F., Lyu, C. and Salva, M., 2019. Soil properties: physics inspired, data driven. In: M. Iskander, K. Villegas and J. Zhang, eds. *Geotechnical fundamentals for addressing new world challenges*. Boca Raton, Florida: CRC Press, pp.67–91. <https://doi.org/10.1201/9780429297530-6>
- Sun, L., Jia, T., Zhuo, R., Yan, S. and Guo, B., 2015. Numerical solutions for consolidation of under-consolidated dredger fill under vacuum preloading. *Journal of Coastal Research*, (73), pp.277–282. <https://doi.org/10.2112/SI73-048.1>
- Vucetic, M. and Dobry, R., 1988. Degradation of marine clays under cyclic loading. *Journal of Geotechnical Engineering*, 114(2), pp.133–149. [https://doi.org/10.1061/\(ASCE\)0733-9410\(1988\)114:2\(133\)](https://doi.org/10.1061/(ASCE)0733-9410(1988)114:2(133))
- Wichtmann, T., 2005. Explicit accumulation model for non-cohesive soils under cyclic loading. PhD thesis. Institut für Grundbau und Bodenmechanik, Technische Universität Braunschweig.